Robust Control of Friction-Driven Reconfigurable Adaptive Structures

Alejandro Palacio-Betancur[a], Adam Rácz[b], Mohammad Ali Maghsoudlourad[b], Viacheslav Slesarenko[b], and Mariantonieta Gutierrez Soto[c]

[a]Department of Civil and Environmental Engineering, The Pennsylvania State University, 212 Sackett Building, University Park, PA 16802 U.S.A. ORCID: https://orcid.org/0000-0003-3189-3406

[b]Cluster of Excellence livMatS @ FIT - Freiburg Center for Interactive Materials and Bioinspired Technologies, University of Freiburg, Georges-Köhler-Allee 105, Freiburg im Breisgau, 79110 Germany

[c]School of Engineering Design and Engineering, 307 Engineering Design and Innovation Bldg., Pennsylvania State University, University Park, PA 16802 U.S.A., with corresponding author email. Email: mvg5899@psu.edu. ORCID: https://orcid.org/0000-0003-1609-5801

ABSTRACT

Traditional design methods for engineering applications aim to achieve optimal performance for specific conditions or moderate performance for a broader range of conditions. However, the optimal performance for a wide spectrum of situations can be facilitated if such systems possess reconfiguration capability. It can be illustrated in the example of structures with steerable joints, which is a popular approach in robotics. By rotating the joints to a different degree, a plethora of resulting configurations can be achieved – configurations that might be specifically suited for the required conditions. Systems based on these principles can be implemented on the macroscopic level in adaptive facades, on the mesoscopic level in mechanical metamechanisms, and at the microscopic level in microelectromechanical devices. In general, adaptive structures often require numerous actuators to facilitate a wide range of reachable configurations, leading to increasing energy demands as the system size increases. This can be seen in the case of robotics when each joint can be independently actively rotated to drive the motion corresponding to the specific degree of freedom. This paper analyzes an alternative situation, when the joins are semi-active and can exist only in either a locked or unlocked state, with only one (last joint) being actively steered. In the ideal case, the energy should be consumed only for switching between states, while maintaining the state should be free with locking achieved via switchable friction. While theoretically improving energy efficiency, such a system makes it much more challenging to control the resulting shape of the structure as compared with its counterpart with actively rotating joints. In this paper, we develop a motion planning algorithm to facilitate the achievement of the desired shape via control over the state of the joints and the position of the last link. In particular, the change of shape is performed by a sequence of single-degree-of-freedom motions determined by a motion planning algorithm based on Rapidly exploring Random Trees and sub-slider-crank systems (RRT-SC). One application of the proposed method is evaluated for reconfigurable building facades and paves the way for the next generation of structures in smart cities.

Keywords: Robust control, adaptive structures, adaptive architecture, motion planning, tracking control, reconfigurable

1. INTRODUCTION

Depending on the design goal, engineers might opt for one of two options: create systems that are extremely good for a very narrow range of conditions and do not work beyond this range (typical for metamaterials[1,2]), or systems

Further author information: (Send correspondence to M.G.S.)
M.G.S.: E-mail: mvg5899@psu.edu

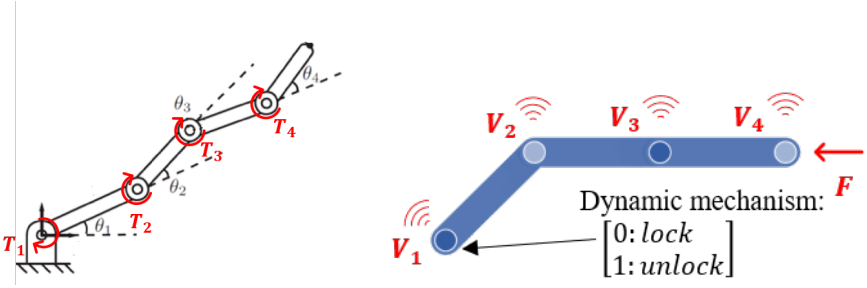
Behavior and Mechanics of Multifunctional Materials XVIII, edited by Aimy Wissa, Mariantonieta Gutierrez Soto, Russell W. Mailen, Proc. of SPIE Vol. 12947, 129470F · © 2024 SPIE · 0277-786X · doi: 10.1117/12.3010949

that are averagely good across a broader range of conditions. Reconfiguration capacity enriches the potential of structures to deliver good performance regardless of external circumstances. Reconfiguration along with sensing and processing are the three key pillars of adaptivity – the trait that transpires in living materials. The concept of reconfiguration on the fundamental level is tightly connected to the idea of "mechanism" – a system consisting of multiple parts connected in a specific fashion. In many cases, mechanics can be described as a system containing rigid elements separated by the joints where the rotation or linear motion is possible. Rotation in the joints can be either actively driven by the actuator inside of the specific joint or by motion of the neighboring elements.[3] Under this umbrella term, one might put the systems existing on different length scales: from macroscopic adaptive facades[4–6] via mesoscopic metamaterial-based mechanisms[7,8] to microelectromechanical devices (MEMS) on a microscopic level.[9,10] A higher number of active actuators or joints enables a wider state space, however, energy input scales exponentially with the length scale of the system. Therefore, systems similar to MEMS digital micromirror devices[11] with hundreds of thousands of independent active elements are not feasible on a macroscale. Due to that, complex mechanisms on the mesoscale and macroscale usually use less active elements and have to harness interaction between them to achieve the desired functionality, which is not a trivial control task. Normally, the reconfiguration is not required to be performed very frequently, so the majority of the time the system exists in standby mode. However, if electrical components such as motors are used in joints for their rotation, even in the standby mode, the system still consumes energy. An alternative solution relies on semi-active joints that can switch between open and closed states using energy only for switching. In this case, joints can employ different physics, in particular utilizing switchable friction or bistable elements.[12] In this paper, we adopt this approach and develop a strategy for controlling the resulting shapes of 1D chain-like mechanisms with semi-action friction-based joints applying them to the adaptive architecture concept.

2. METHODOLOGY

2.1 Proposed mechanical system

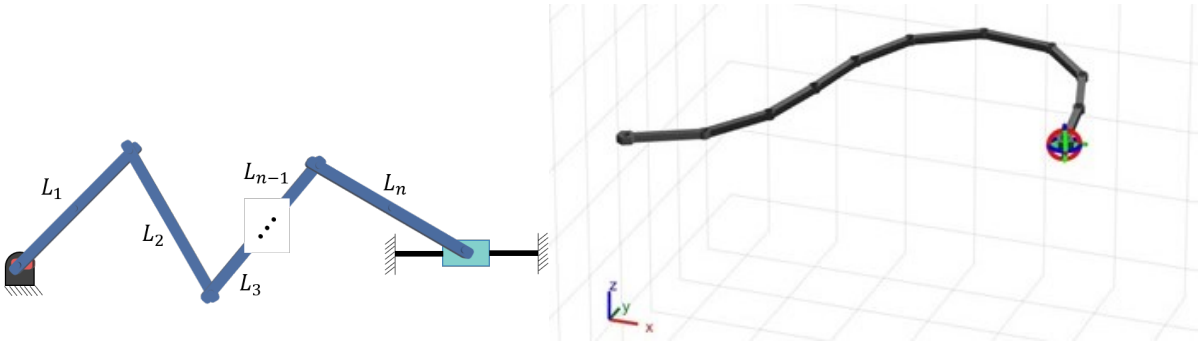
A mechanism is formed by connecting rigid bodies (links) with joints that allow a relative movement between adjacent links (Fig. 1a). To cause the mechanism to move it is necessary to make one or multiple joints active. Usually, these system allows a fast change of shape if all of the joints actively rotate using already developed motion planning and control algorithm.[13] However, to minimize the energy consumption and potentially simplify the joint design, in the considered system, the motion is prescribed only on the last link in the chain in the form of linear translation in the horizontal direction as shown in Fig.1b. Simultaneously, the remaining joints can dynamically switch between locked and unlocked states. In an unlocked state, the rotation of the connecting links is free, while if the joint is in the locked state, the system loses one degree of freedom.



(a) (b)

Figure 1: Actuation system for rigid links and rotational joint system (a) Conventional approach (b) Proposed approach

The proposed mechanical system can be classified as a serial closed kinematic chain with n links as shown in Fig. 2a. This system has a total of $n-1$ degrees of freedom and a single actuator. Therefore, conventional motion planning algorithms will not guarantee an accurate shape change, especially if the number of links increases. In addition, the speed of change of shape is lower compared to the conventional approach with several actuators. Therefore, there is a need for a new efficient motion planning algorithm for this proposed mechanism.



(a) (b)

Figure 2: Proposed mechanical system (a) Concept (b) URDF of reconfigurable system

The following sections focus on the development of components necessary to achieve an autonomous change in the shape of the system. These include a new motion planning algorithm, physics-based modeling, real-time image-based measurements, tracking control, and prototypes of the locking mechanism. For these developments, it was necessary to understand the kinematics of mechanisms that are formed with rigid bodies and rotational joints. A Unified Robotic Description Format (URDF) model was generated using MATLAB to understand joint configurations with inverse kinematics as shown in Figure 2b.

2.2 Proposed motion planning algorithm

The conventional motion planning algorithms will not guarantee an accurate change of shape because the number of degrees of freedom (*n-1*) is higher than the number of actuators (m), especially if the number of links increases. A complete motion of any system requires that the degrees of freedom are equal to the number of actuators. This means that it is possible to leverage the use of the dynamic lock/unlock mechanism to reduce the degrees of freedom from *n-1* to m, and sequentially control the shape of the system. If the system only has one actuator, this approach is known as the "effective crank-slider"[14] because it reduces the system to a generic slider-crank mechanism with a single degree of freedom as shown in Fig. 3. The selection of consecutive

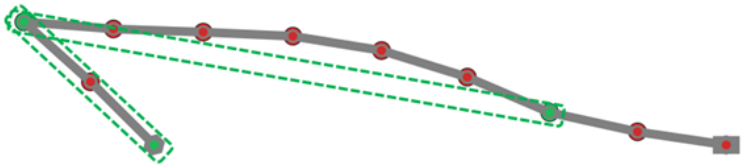


Figure 3: Reduction of degrees of freedom with locking mechanisms to generate an effective slider-crank mechanism. The **red** joints are locked and **green** joints are unlocked

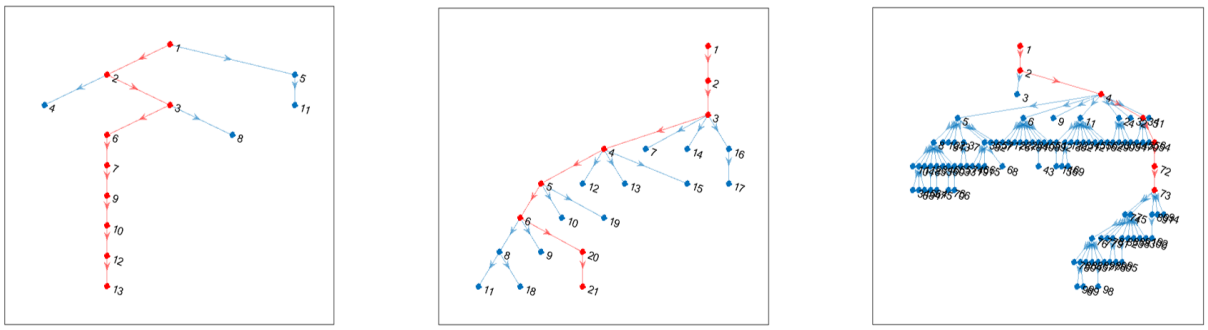
steps is not a straightforward task because the amount of possible sequences is equal to $(n-1)!/(n-4)!$. In addition, these types of systems can achieve configurations where two links are co-linear, meaning that they reach an extremely extended or contracted position. This is known as a toggle position, and they can be problematic from the motion planning perspective because they are unpredictable.[15] To address these challenges, the new proposed motion planning algorithm combines the principles of the "effective crank-slider" with a well-established exploration algorithm known in robotics as the Rapidly-exploring Random Trees (RRT).[16] The proposed algorithm is denominated as *RRT-SC* and the idea is to find the sequence of steps required to achieve a desired shape while avoiding toggle positions. The pseudo-code of this method is shown in Algorithm 1.

The proposed algorithm can randomly choose configurations from G to generate the next branches of the graph. This random selection and generation control the exploration and exploitation of the algorithm as shown in Fig. 4. Each node represents a vertex of the graph G with configuration q_i, and each line is a vertex of G that represents the transition between configurations. The first version exploits good configurations and reaches the

Algorithm 1: RRT-SC algorithm

Data: initial configuration q_{init}, final configuration q_{end}
Result: graph G with path between q_{init} and q_{end}
$q_{new} \leftarrow q_{init}$;
$G.init \leftarrow q_{new}$;
while $q_{new} \neq q_{end}$ **do**
  Choose an existing configuration from G, q_0;
  Generate an effective slider-crank (unlock 3 joints);
  Adjust angle on the first joint and generate q_{new};
  if *Angle doesn't cross toggle position* **then**
    $G.addvertex(q_{new})$;
    $G.addedge(q_0, q_{new})$;
  else
    Generate q_{new} right before reaching toggle position;
    $G.addvertex(q_{new})$;
    $G.addedge(q_0, q_{new})$;
  end
end

goal fast, however, convergence may not be guaranteed. Contrarily, the third version does excessive exploration to find the optimal path but it requires more computational efforts. Therefore, the second version is balanced in both aspects. Thus, the final proposed algorithm has a balanced behavior that reduces computational time and avoids redundancies because it chooses configurations "close" to the final configurations to generate the new branches, and generates four effective slider cranks from this configuration.



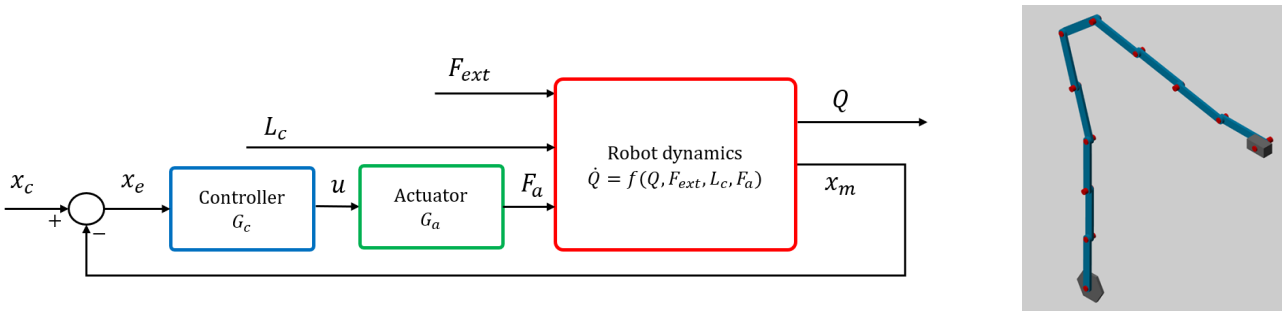
(a) (b) (c)

Figure 4: Exploration vs Exploitation for graph G(a) High exploitation (b) Balanced exploration and exploitation (c) High exploration

2.3 Joint space motion model

Once the sequence of motions is established by the *RRT-SC* algorithm, the next step is to guarantee a smooth trajectory between steps to transition between shapes according to the capabilities of the actuator, the external forces applied on the system, and the locking forces generated by the joints. For this purpose, a physics-based model that incorporates these components was generated using Simscape in MATLAB SIMULINK. The simplified block diagram of the system is shown in Fig. 5a,

Where $Q = [q; \dot{q}]^\intercal$ is the state vector of the dynamic system, q is the vector of angles of the system, x_c is the command displacement of the actuator, x_m is the measured displacement of the actuator, x_e is the error



(a) (b)

Figure 5: Physics-based model (a) Block diagram and (b) Preview

between command and measured displacement, u is the command to the actuator, G_c is the controller that will be described in detail in section 2.4, G_a is the actuator dynamics, F_{ext} is the matrix of external forces applied on the rigid body, L_c is the locking command vector, F_a is the force applied by the actuator to the system, and $f()$ is the function of rigid body dynamics defined as:

$$\dot{Q} = \begin{bmatrix} \dot{q} \\ \mathbf{M}(q)^{-1}(-\mathbf{C}(q,\dot{q})\dot{q} - \mathbf{G_t}(q) - \mathbf{J}(q)^{\intercal}(F_{ext} + L_c F_{loc} + F_a)) \end{bmatrix} \tag{1}$$

where $M(q)$ is the joint-space mass matrix, $C(q, \dot{q})$ are the Coriolis terms, $G_t(q)$ are the gravity torques and forces, $J(q)$ is the geometric Jacobian for the specified joint configuration, and F_{loc} is locking force provided by the mechanism discussed in section 2.5. Based on this modeling approach, a preview of the system can be generated as shown in Fig. 5b.

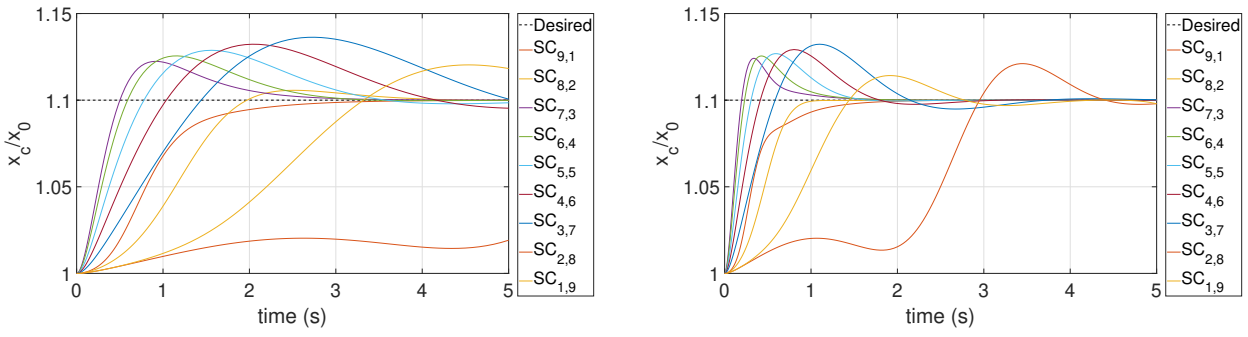
2.4 Tracking control of actuator

The tracking controller G_c shown in 1 defines the command to the actuator to produce a force output of the actuator to move the reconfigurable system towards the command displacement x_c. The proposed controller consists of a proportional-integral-derivative (PID) controller[17] as follows:

$$u = G_c(K_p, K_i, K_d, x_e) = -K_p x_e - K_i \int x_e - K_d \dot{x_e} \tag{2}$$

where K_p, K_i, and K_d are the proportional and derivative gains of the controller. Since the change of shape of the reconfigurable system has a sequence of sub-slider-crank systems, each one with different lengths and distribution of masses, the controller gains need to be defined in a way that they guarantee accurate trajectories for a range of slider-crank geometrical properties. As an example of the challenges for the controller, if the system has 10 links ($n = 10$), with unitary length and mass density, the dynamics of the actuator are simplified as $\ddot{F}_a = u$, the PID gains are $K_p = 100$, $K_i = 100$, and $K_d = 10$, the initial actuator location (x_0) is randomly selected and the command displacement ($x_c = 1.1x_0$), the response of nine sub-slider-cranks ($SC_{a,b}$) with links lengths (a and b) varying from 1 to 9, are shown in Fig. 6a.

The responses shown in Fig. 6a show a clear difference of accuracy when the sub-slider-crank mechanism changes geometric properties. There are cases where the response is slower than others, this may be acceptable in some practical cases where the change of shape can take longer. However, there are cases where this compromises the sequence of steps provided by the $RRT - SC$ algorithm. Thus, there needs to be a more careful selection of PID gains according to the range of geometrical properties of the reconfigurable system. After trial and error, if the gains are chosen as $K_p = 500$, $K_i = 1000$, and $K_d = 18$, a better response is guaranteed, providing more robustness to this type of variation.



(a) (b)

Figure 6: Step response of sub-slider-crank mechanisms for (a) Inaccurate gains and (b) Robust gains

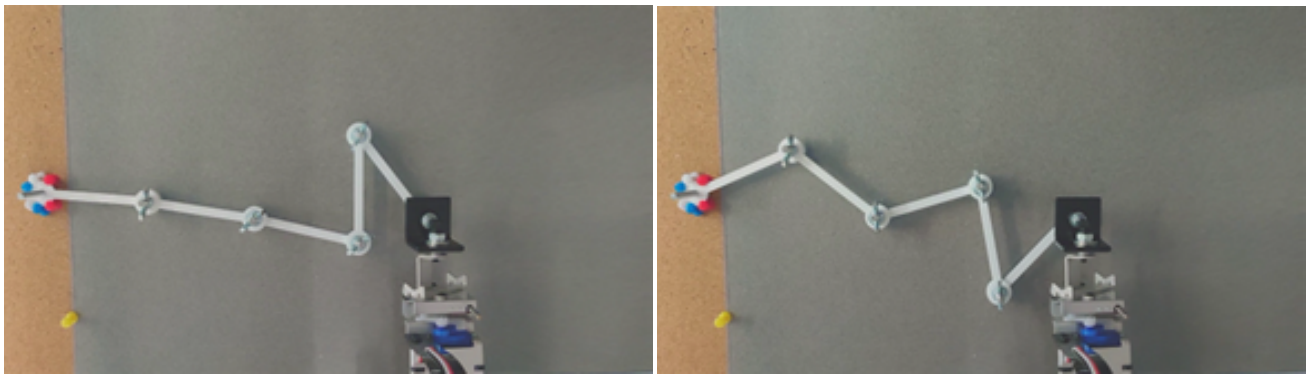
2.5 Proposed locking mechanisms

In general, the semi-active joints can be classified into two categories depending on the locking principles: mechanical[18–20] and friction-driven.[21–24] The first category relies on the permanent mechanical interlocking between two rigid bodies and can be found in latches, ratchets, and dog clutches. Friction-driven locking relies on the contact between the surfaces of two bodies. Among the most common types of mechanisms relying on surface-to-surface contact, one might name, for instance, disc brakes, activated hydraulically.[25] While joints relying on mechanical locking usually require sophisticated geometry or parts, friction-based devices are much easier from a design point of view. Simultaneously, interlocking between two rigid bodies is more robust and usually can withstand higher forces compared with friction-based joints.[26] Since the force of friction generally depends on the normal force applied to the surfaces, relatively high forces need to be generated in the normal direction to increase the friction force and arrest the motion in the hinge. At the same time, compared with mechanical clutches, friction-based locking devices can be stopped at every possible position, which is important for applications in which having a discrete number of fixed joint positions is not a viable option. Therefore, there is a clear trade-off between the design/control complexity and versatility of the locking hinges. Another important aspect of the active locking joints is associated with the activation principle itself. If the friction-based locking principle is selected, then, as mentioned before, the normal force should be high enough to lock the joint in place. Therefore, some kind of force amplifier (mechanical lever) is often required, making the design and fabrication of miniature friction-based locking devices challenging.

To imitate the mechanism described earlier, at the beginning, we used manual adjustment of the bolts located at the joints between straight beams as shown in Figure 7. As one might see, the resulting shape of the chain-like device for the same position of the horizontally moving stage depends on the state of the joints (locked/unlocked). It shows the feasibility of our approach with 1D systems with multiple locking/unlocking elements. For transition to the electronically activated system, we used a locking mechanism based on servomotor as shown in Fig 8. In the unlocked state, the ends of the neighboring beams do not touch allowing them to rotate freely. However, when the servomotor is energized, its rotation leads to the contact between the beam's ends resulting in their inability to move independently, fixing the angle between beams. With this setup, the locking and unlocking can be triggered on demand via a simple microcontroller. We need to note, that this particular realization of the friction-driven joint is not very efficient, since the servomotor has to be energized all the time to hold locked states. We believe, that with slight modification of the mechanism, it is possible to achieve stability of both states (locked and unlocked) without keeping the joint energized. In the current state, the developed principle is used to demonstrate the possibility of controlling the shape utilizing only semi-active joints as opposed to joints that can actively rotate.

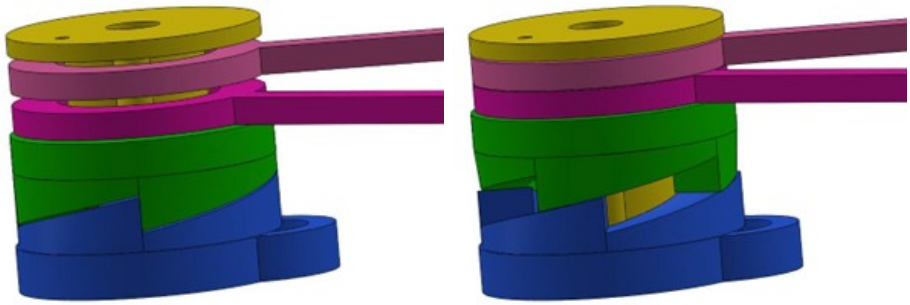
The whole system shown in Fig. 9 was assembled from four active hinges and attached to the linear stage that can move horizontally. The control over the state of the joint was realized using a home-built system incorporating FT232H and PCA9685 boards for I2C communication between the PC and each joint. Green markers were placed on the top of each joint to simplify tracking described in the section 2.6. The resulting shape of the chain-like structure depends on the status of the hinges. Multiple different resulting shapes were achieved

for the same position of the linear stage. The switch between states can be performed during the motion itself, enabling the implementation of path-finding methods developed in 2.2. In addition, the demonstrated system provides an opportunity to introduce defects (broken hinges) on demand to assess the capacity of the system to compensate for mistakes, which will be done in the future using either visual tracking or P2P communication between node-hinges for large-scale systems.



(a) (b)

Figure 7: Different resulting configurations for the same position of the linear actuator demonstrate the feasibility of using locking hinges for the programming of the shape of the chain-like structure.

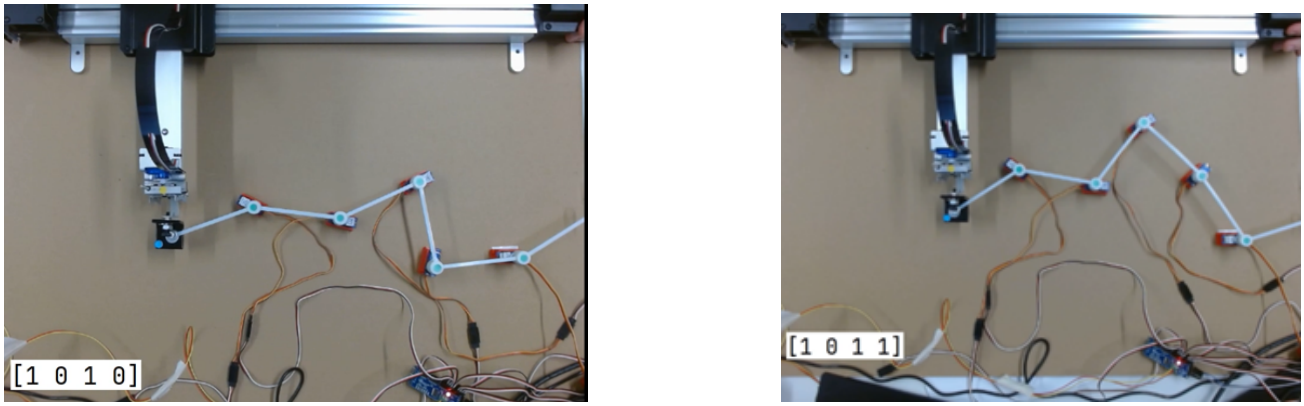


(a) (b)

Figure 8: The locking principle of the device is based on the rotation of the internal shaft (yellow). The unlocked state (left) occurs then the inclined surfaces are in direct contact. After counter-clock rotation, the green moving ring compresses the beams facilitating pressure-driven locking (right).

2.6 Tracking system via image processing

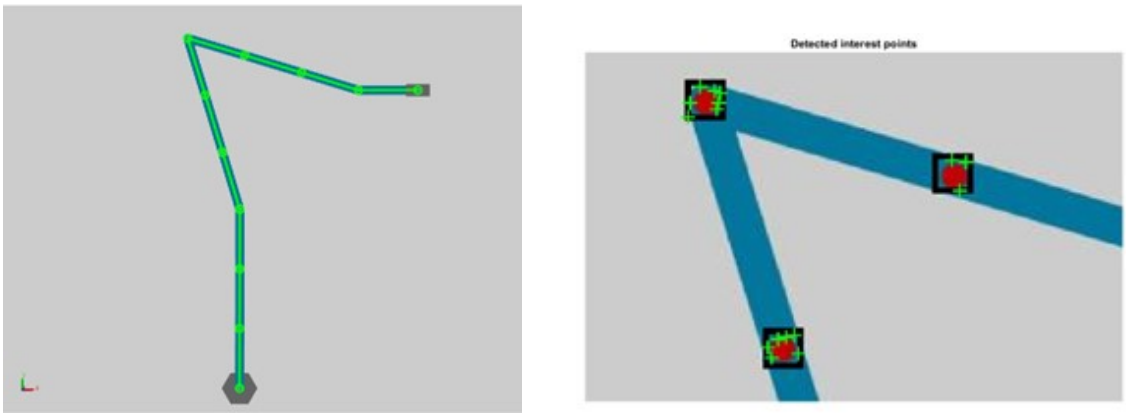
Since the system requires several steps to change the shape, it is necessary to measure in real-time if the joints are achieving the desired locations during motion to avoid undesired shape results or cumbersome shapes that have toggle positions. For this purpose, two image-based algorithms were developed to measure the location of joints and the angle between links. The first algorithm is a static measurement of these properties, and the second is a continuous measurement that is useful to avoid reaching toggle positions or to avoid collisions. The first algorithm takes a picture of the system at a specific instant and finds the positions of markers that are placed at the joints of the reconfigurable system. Then, the distance between markers is computed and according to the length of the links, the sequence of nodes is assigned from the fixed base to the slider node as shown in Fig 10a. After obtaining the corresponding initial and final node of each link, the angle of the joints can be computed and compared to the desired angles determined on a specific step of the motion planning algorithm.
For continuous measurement, it is required to define regions of interest (ROI) based on the markers placed on the locking mechanism, this is achieved by finding circles on the image and the ROI is rectangles on each joint as



(a) (b)

Figure 9: Sample prototype of 1D chain with four active joints. The green markers are placed on the top for the tracking system. Four digits (1 and 0) in the bottom left corner represent the state of each joint (1 – locked, 0 – unlocked).

shown in Fig. 10b. Inside each ROI a series of points of interest are defined near the edges of the markers, and then the Kanade-Lucas-Tomasi (KLT) feature tracker algorithm records the location of these points while the system is moving. The values inside each ROI are average to obtain an approximate location and displacement of the joints. Then, these values are used to compute joint angles and impose conditionals to avoid obstacles or toggle positions during the motion of the system. The systems showed very reliable tracking in the virtual setup, and in the future will be adopted for the real setup shown in Fig. 9.



(a) (b)

Figure 10: Displacement tracking algorithms a) Static measurement b) ROI for continuous measurement

As an example, Fig 11 compares the command angles and the measured angle with the proposed algorithm for a shape change from a triangle to a square shape. There are some minor discrepancies in joints 10 and 11 due to the lack of edges inside the region of interest from the video of the simulation.

3. RESULTS AND DISCUSSION

To demonstrate the applicability of the developed system, we consider its usage as a prototype of adaptive facade.[5] Specifically, we consider the opportunity to modify the corners of the buildings to, for instance, improve the aerodynamic performance.[27,28] A set of 7 minor corner modifications shown in Fig. 12 were generated with 10 links to demonstrate the potential of the proposed methodology. Between these generated shapes, it is possible to choose 42 pairs and generate a sequence of motions to transition in between them. The proposed

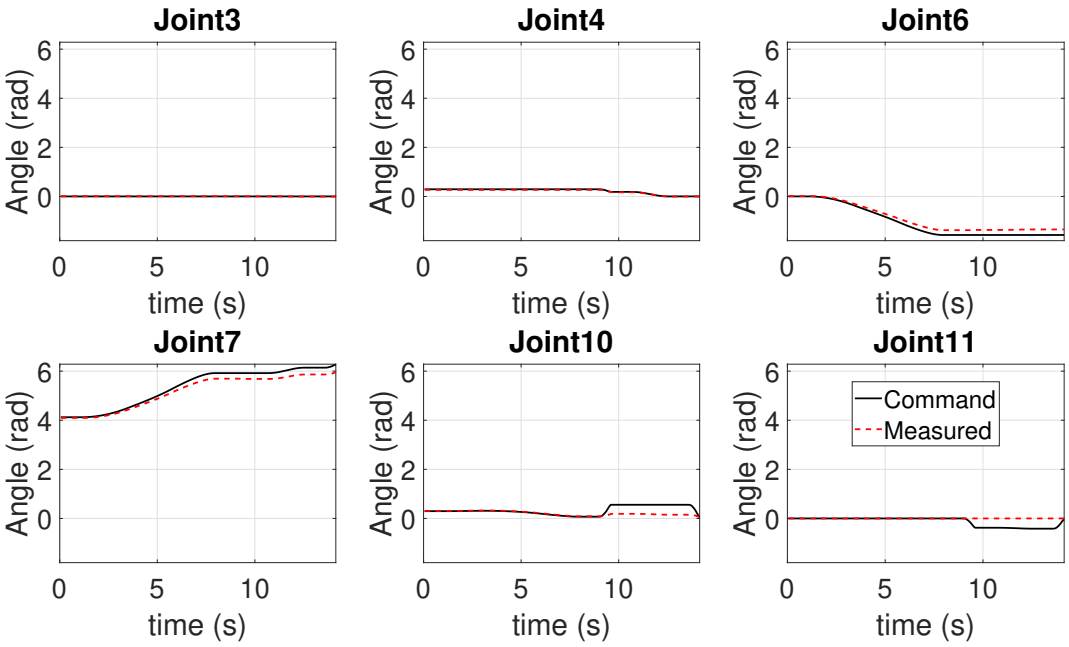


Figure 11: Results of continuous motion tracking of the proposed reconfigurable system

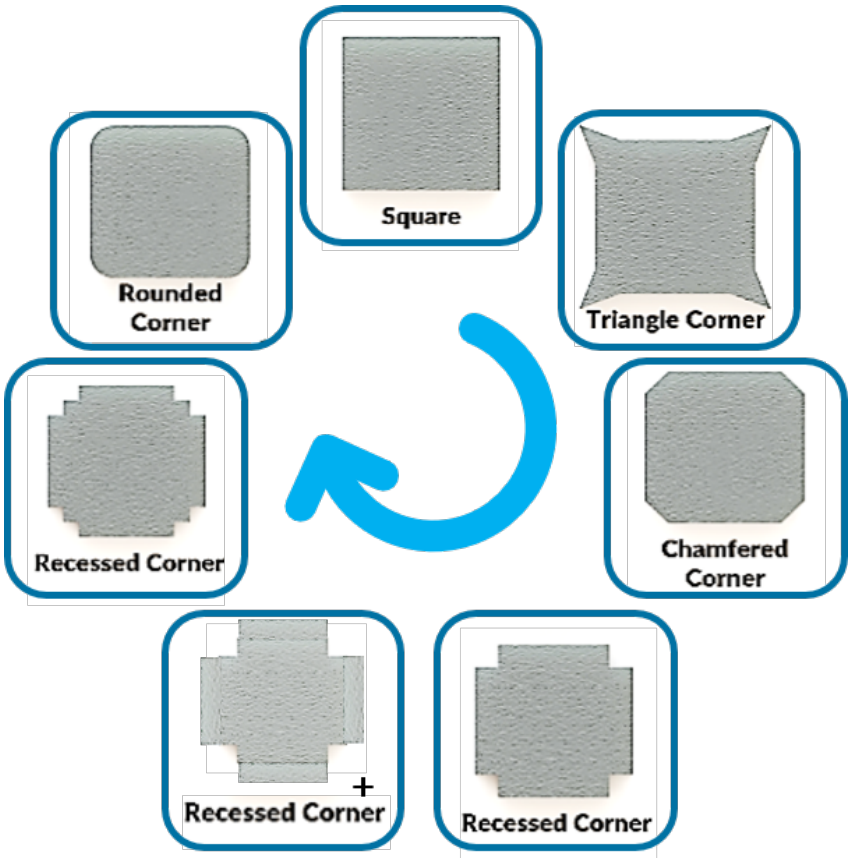


Figure 12: Desired minor corner modifications

algorithm was implemented for all scenarios and it successfully found a path for. As an example, Fig. 13 shows the sequence of steps found by the algorithm to transition between a big recessed corner and a small recessed corner. The red and green circles indicate locked and unlocked joints, respectively, the green dotted line shows the effective slider-crank mechanism and the force F shows the direction of motion. This example only required four steps to reach the final configuration.

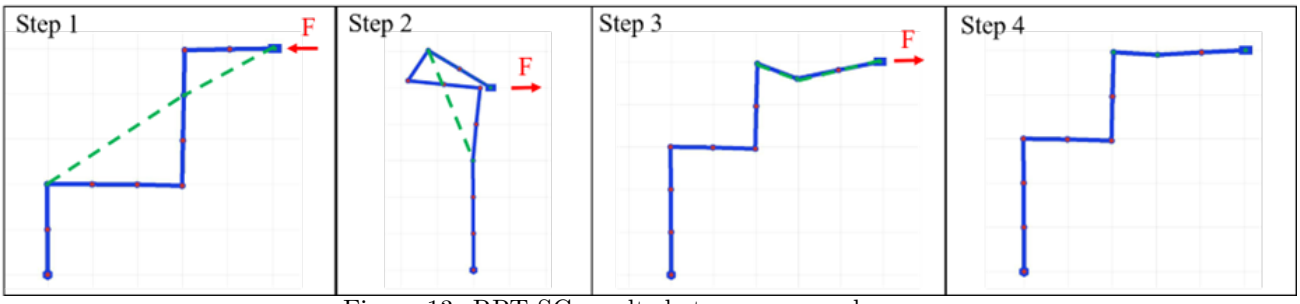


Figure 13: RRT-SC results between recessed corners

Since this system is intended to be placed on a corner of a building, obstacle detection was added as a feature to the motion planning algorithm to avoid collision of links against the building. Fig. 14 shows the sequence of steps found by the algorithm to transition between the small recessed corner and the big recessed corner without touching the gray area that symbolizes the building.

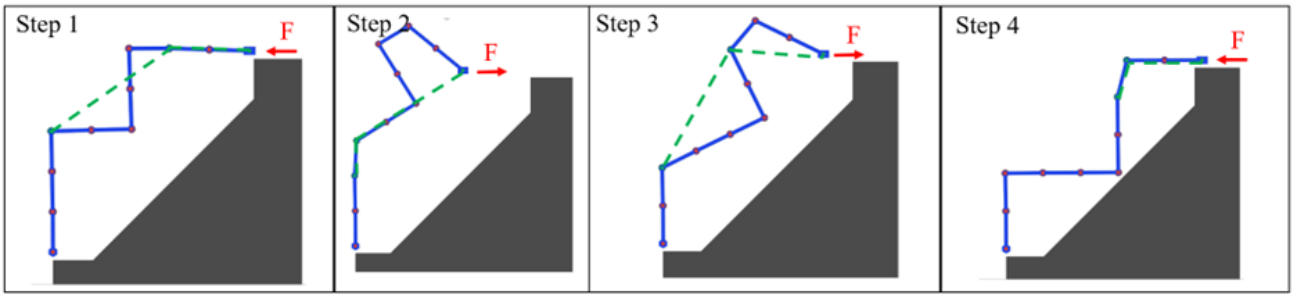


Figure 14: RRT-SC results including obstacle detection

Fig. 15 shows another example of corner modification between a triangle and square corners. Similar to the previous two examples, it required a few steps to find the final configuration. For these steps, there were three sub-slider-crank mechanisms with different lengths. Using the joint space motion model shown in Fig. 6, the robust PID controller designed in section 2.4, under the assumptions of unitary mass density, unitary link lengths, and simplified actuator dynamics, the displacements shown in Fig. 16 were obtained.

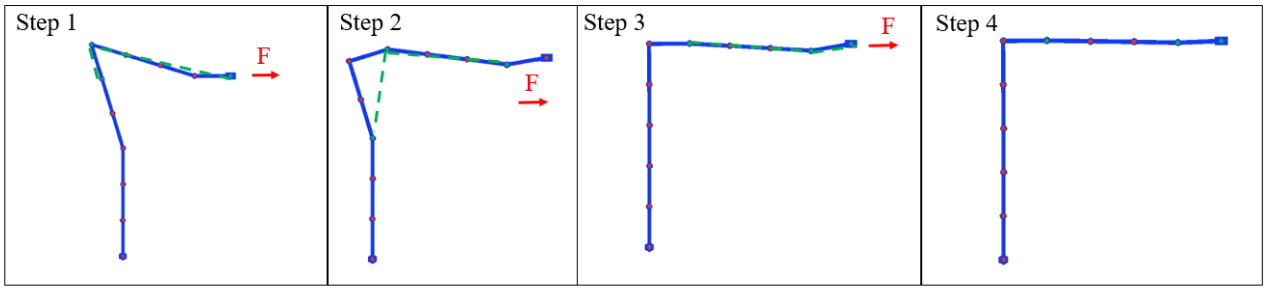


Figure 15: RRT-SC results between triangle and square

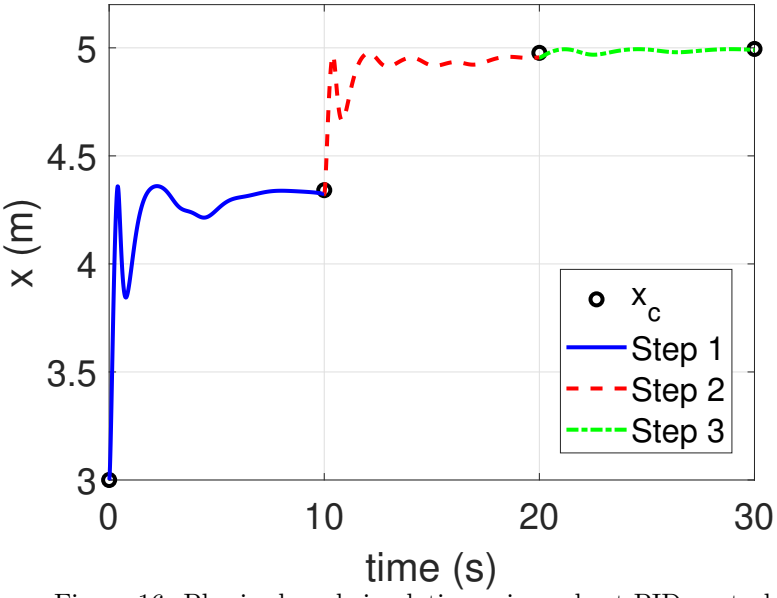


Figure 16: Physics-based simulation using robust PID control

The error displacements using 10 seconds of simulation for each step, were 0.018, 0.0206, and 0.0049 units, respectively. If the length of each link is 1, this can be considered as a negligible error, and tracking displacement provided enough accuracy to change the shape between triangle and square corners.

Based on these results, the recommended sequence of steps to use the proposed methodology is:

1. Define initial ($q_{initial}$) and final configurations (q_{end}),
2. Design a robust PID controller based on robot and actuator dynamics,
3. Find a sequence of steps between configurations using the RRT-SC algorithm from section 2.2,
4. Use the displacement command (x_c) and corresponding locking commands (L_c) to move the system to the first step,
5. Use the continuous image-based tracking system to monitor obstacle collisions (stop motion in case of proximity with objects),
6. If the system reaches the desired displacement, take a photo with a camera, and perform the static angle measurement shown in Fig. 10b
7. Compare measured angles with desired angles from RRT-SC at the first step:
   (a) If the difference is small (less than a threshold), the motion continues
   (b) If the difference is large, re-planning needs to take place using the final configuration as the new initial configuration.

4. CONCLUSIONS AND FUTURE WORK

The proposed methodology, including dynamic locking mechanisms, motion planning algorithms, physics-based modeling, robust tracking control, and image-based measurements enables new technologies for reconfigurable structures that can be applied at different length scales. The proposed motion planning algorithm can be generalized to any number of links and desired shapes, however, the computational demand for a large number

of elements needs to be studied to evaluate feasibility for small-scale applications that could require more elements than meso- and macro-scales. In addition, a single PID controller may not be feasible for all the possible sub-slider-crank mechanisms inside a system with a large number of elements, therefore, new control strategies would need to be studied such as gain scheduling and adaptive controllers.[29] In general, the physical prototypes for the proposed reconfigurable system at the current stage cannot be classified as energy-efficient due to the need for holding power during locking. Future work includes modification of the proposed mechanisms that will have two stable states. A brief review of the energy efficiency of other possible locking friction-based systems has been performed, showing the necessity of a compromise between energy requirements and achieving the minimal force needed for robust locking. Additional interest includes evaluating the load-bearing capability and real-time adaptation facing environmental loading conditions.

ACKNOWLEDGMENTS

The authors acknowledge the support of the Convergence Center for Living Multifunctional Material Systems (LiMC2) and the Cluster of Excellence Living, Adaptive and Energy-autonomous Materials Systems (livMatS) Living Multifunctional Materials Collaborative Research Seed Grant Program. VS, AR, and MAM acknowledge funding by Deutsche Forschungsgemeinschaft (DFG, German Research Foundation) under Germany's Excellence Strategy – EXC-2193/1 – 390951807 and by the Carl Zeiss Foundation (Research cluster "Interactive and Programmable Materials - IPROM"),

REFERENCES

[1] Surjadi, J. U., Gao, L., Du, H., Li, X., Xiong, X., Fang, N. X., and Lu, Y., "Mechanical Metamaterials and Their Engineering Applications," *Advanced Engineering Materials* **21**(3), 1800864 (2019).

[2] Cummer, S. A., Christensen, J., and Alù, A., "Controlling sound with acoustic metamaterials," *Nature Reviews Materials* **1**(3), 1–13 (2016).

[3] Wittenburg, J., [*Kinematics*], Springer, Berlin, Heidelberg (2016).

[4] Attia, S., Lioure, R., and Declaude, Q., "Future trends and main concepts of adaptive facade systems," *Energy Science & Engineering* **8**(9), 3255–3272 (2020).

[5] Bellamy, A., Boustani, J., Brehm, C., and Gutierrez Soto, M., "Towards resilient adaptive origami-inspired diagrid building envelope," in [*Active and passive smart structures and integrated systems XIII*], **10967**, 288–298, SPIE (2019).

[6] Hou, F., Sarkar, P. P., and Alipour, A., "A novel mechanism - smart morphing façade system - to mitigate wind-induced vibration of tall buildings," *Engineering Structures* **275**, 115152 (2023).

[7] Ion, A. and Baudisch, P., "Metamaterial devices," in [*ACM SIGGRAPH 2018 Studio*], *SIGGRAPH '18*, 1–2, Association for Computing Machinery, Vancouver, British Columbia, Canada (2018). 00000.

[8] Ion, A., Wall, L., Kovacs, R., and Baudisch, P., "Digital Mechanical Metamaterials," in [*Proceedings of the 2017 CHI Conference on Human Factors in Computing Systems*], *CHI '17*, 977–988, Association for Computing Machinery, New York, NY, USA (2017).

[9] Kota, S., Joo, J., Li, Z., Rodgers, S. M., and Sniegowski, J., "Design of compliant mechanisms: applications to mems," *Analog integrated circuits and signal processing* **29**, 7–15 (2001).

[10] Xiao, S., Wang, T., Liu, T., Zhou, C., Jiang, X., and Zhang, J., "Active metamaterials and metadevices: a review," *Journal of Physics D: Applied Physics* **53**(50), 503002 (2020). Publisher: IOP Publishing.

[11] Ren, Y.-X., Lu, R.-D., and Gong, L., "Tailoring light with a digital micromirror device," *Annalen der physik* **527**(7-8), 447–470 (2015).

[12] Plooij, M., Mathijssen, G., Cherelle, P., Lefeber, D., and Vanderborght, B., "Lock your robot: A review of locking devices in robotics," *IEEE Robotics & Automation Magazine* **22**(1), 106–117 (2015).

[13] Lynch, K. M. and Park, F. C., [*Modern robotics*], Cambridge University Press (2017).

[14] Christoforou, E. G., Müller, A., Phocas, M. C., Matheou, M., and Arnos, S., "Design and control concept for reconfigurable architecture," *Journal of Mechanical Design* **137**(4), 042302 (2015).

[15] Norton, R., [*Design of machinery*] (1998).

[16] LaValle, S., "Rapidly-exploring random trees: A new tool for path planning," *Research Report 9811* (1998).

[17] Gutierrez Soto, M. and Adeli, H., "Recent advances in control algorithms for smart structures and machines," *Expert Systems* **34**(2), e12205 (2017).

[18] Palpacelli, M., Carbonari, L., and Palmieri, G., "A lockable spherical joint for robotic applications," in [*2014 IEEE/ASME 10th International Conference on Mechatronic and Embedded Systems and Applications (MESA)*], 1–6 (2014).

[19] Collins, S. H. and Kuo, A. D., "Recycling Energy to Restore Impaired Ankle Function during Human Walking," *PLOS ONE* **5**(2), e9307 (2010). Publisher: Public Library of Science.

[20] Wright, C., Buchan, A., Brown, B., Geist, J., Schwerin, M., Rollinson, D., Tesch, M., and Choset, H., "Design and architecture of the unified modular snake robot," in [*2012 IEEE International Conference on Robotics and Automation*], 4347–4354 (2012). ISSN: 1050-4729.

[21] Controzzi, M., Cipriani, C., and Carrozza, M. C., "Miniaturized non-back-drivable mechanism for robotic applications," *Mechanism and Machine Theory* **45**(10), 1395–1406 (2010).

[22] Shin, D., Yeh, X., and Khatib, O., "A new hybrid actuation scheme with artificial pneumatic muscles and a magnetic particle brake for safe human–robot collaboration," *The International Journal of Robotics Research* **33**(4), 507–518 (2014). Publisher: SAGE Publications Ltd STM.

[23] Chou, J. B., Yu, K., and Wu, M. C., "Electrothermally Actuated Lens Scanner and Latching Brake for Free-Space Board-to-Board Optical Interconnects," *Journal of Microelectromechanical Systems* **21**(5), 1107–1116 (2012). Conference Name: Journal of Microelectromechanical Systems.

[24] Slesarenko, V. and Pastewka, L., "The bumpy road to friction control," *Science* **383**(6679), 150–151 (2024).

[25] Orthwein, W. C., [*Clutches and Brakes: Design and Selection*], CRC Press, Boca Raton, 2 ed. (2004).

[26] Plooij, M., Mathijssen, G., Cherelle, P., Lefeber, D., and Vanderborght, B., "Lock Your Robot: A Review of Locking Devices in Robotics," *IEEE Robotics & Automation Magazine* **22**(1), 106–117 (2015). Conference Name: IEEE Robotics & Automation Magazine.

[27] Ding, F., Kareem, A., and Wan, J., "Aerodynamic tailoring of structures using computational fluid dynamics," *Structural Engineering International* **29**(1), 26–39 (2019).

[28] Elshaer, A., Bitsuamlak, G., and El Damatty, A., "Enhancing wind performance of tall buildings using corner aerodynamic optimization," *Engineering Structures* **136**, 133–148 (2017).

[29] Palacio-Betancur, A. and Gutierrez Soto, M., "Recent advances in computational methodologies for real-time hybrid simulation of engineering structures," *Archives of Computational Methods in Engineering* **30**(3), 1637–1662 (2023).